Earth and Space Science

Effects of Solar Variability on Tropical Cyclone Activity

Chinmaya Nayak[1] , **Jayashree Bulusu[1], Geeta Vichare[1]** , **and A. P. Dimri[1]**

[1]Indian Institute of Geomagnetism, Navi Mumbai, India

Abstract The current study explores the relationship between solar variability and tropical cyclone (TC) activity using sunspot number (SSN) and TC best-track data as respective proxies. We have considered six regions of the globe, for example, EP: Eastern Pacific, NA: North Atlantic, NI: North Indian, SI: South Indian, SP: South Pacific, and WP: Western Pacific. The results show strong anti-correlation between yearly TC activity and yearly SSN while considering their 11-year moving averages. This behavior is consistent for TC counts as well as accumulated cyclone energy. However, this is true only for the North Atlantic region. Overall, when we consider all regions together, more TCs (in terms of counts) are observed during lower solar activity periods (SSN < 50) as compared to higher solar activity conditions (SSN > 100). However, the yearly rates remain more or less similar. On the other hand, extreme TC events with a maximum wind speed of 137 knots and higher (category 5) are most likely to occur during the declining phase of a solar cycle and least likely to occur during the ascending phase or the maximum phase. Although solar activity levels are similar during the declining and ascending phases, the yearly occurrence rate is nearly double in the declining phase (1.123) as compared to that in the ascending phase (0.625).

1. Introduction

Over the past few decades, substantial progress has been made in understanding TC dynamics and prediction (Chan, 2005; Chen et al., 2020; K. Emanuel, 2003; Roy & Kovordányi, 2012; Wang & Wu, 2004, and references therein). Starting from understanding the physics and dynamics to real-time tracking and prediction, the scientific community has done considerable development. However, one aspect that remains a gray area is how solar variability affects TC activity. Cohen and Sweetser (1975) directly looked into a possible relationship between TCs and solar activity. The authors did a spectral analysis of smoothed TC count, TC season length (7-year running averages) for the Atlantic basin, and sunspot number (SSN) (12-month running average) data and suggested a possible relationship between Atlantic TC activity and solar cycle. However, they did not offer any possible mechanism. Further, Ivanov (2007) looked into the correlation between magnetic storms and TC counts for nearly a single solar cycle between 1996 and 2006. The study found that each basin behaved differently. The Atlantic basin showed a positive correlation between the two, whereas the northwestern Pacific and the Southern Hemisphere showed negative correlations. The study found no significant correlation in the northeastern Pacific.

On the contrary, Elsner and Jagger (2008) suggested that inactive sun increases the probability of a U.S. hurricane. The authors developed a statistical model of TC frequency for the Atlantic basin and showed that including SSN as a covariate in the model prompted significant improvements. In follow-up work, Elsner et al. (2010) linked the inverse relationship between TC intensity and solar activity to the variation in temperature at the top of the TC caused by UV radiation during a solar cycle. This is based on the heat engine theory of TCs, which suggests that the TC wind speeds vary inversely with the mean outflow temperature above the cyclone. As a result, an increased air temperature at the top of a TC will decrease cyclone intensity. The high sensitivity of TC warm core to solar short wave radiation was confirmed by Ge et al. (2015). On a different note, using the TC activity index (CAI) from Australia, which is available for the last 1,500 years, Haig and Nott (2016) demonstrated the contribution of solar forcing over decadal, interdecadal, and centennial scales, over Australian TC activity.

Most of the above-mentioned studies mostly used SSN as a proxy for solar activity, without differentiating between contributions from variability in solar irradiance and geomagnetic activity. Several studies looked into how geomagnetic activity affects cyclones. Li et al. (2019) studied the role of solar wind energy flux on the modulation of global TC activity. The authors suggest that the TCs seem to be stronger with more intense geomagnetic disturbances. The results are in stark contrast to those of Elsner et al. (2010), Elsner and Jagger (2008). The authors tried to explain the results based on reduced cosmic ray-driven cloud cover decrease during higher solar

activity conditions which may allow the open oceans to get hotter and provide the necessary potential energy required for TC intensification.

The geomagnetic activity seems to be more effective in modulating extra tropical cyclones (TCs) (Prikryl, Muldrew, & Sofko, 2009; Prikryl, Rušin, & Rybanský, 2009). The authors noted that the advent of HSS/CIRs (high-speed solar wind streams/corotating interaction regions) or ICMEs (Interplanetary Coronal Mass Ejections) was generally followed by extra-tropical storms, wind storms, or winter storms. Prikryl et al. (2016) performed a superposed-epoch analysis of the 530.3-nm solar corona emission line intensity and solar wind plasma parameters to investigate this phenomenon. The results showed that the arrival of HSSs were closely followed by explosively developing extra-TCs, in a significant number of cases. Most of these effects were observed at latitudes poleward of 40°N. A possible mechanism was proposed which was based on the generation of Joule heating and/or Lorentz forcing of the high-latitude ionosphere/thermosphere leading to the generation of atmospheric gravity waves (AGWs). These AGWs can propagate downwards reaching the troposphere and lead to the formation of conditional moist symmetric instability which may in turn contribute toward intensification of extratropical cyclones (Prikryl et al., 2016, 2018; Prikryl, Rušin, & Rybanský, 2009). It is worthwhile to mention here that the above-mentioned work relating extratropical cyclones to HSS/CIRs were partly motivated by the "Wilcox effect" (Roberts & Olson, 1973; Wilcox et al., 1973, 1974, 1976). It relates the tropospheric vorticity (300-–500-hPa levels) and solar wind magnetic structure. As the earth passes through a solar wind magnetic boundary or heliospheric current sheet (HCS), the vorticity area index (Roberts & Olson, 1973) showed a statistically significant decrease, one day after the HCS passage (Hines & Halevy, 1977).

In this study, we revisit the topic of relationship between TCs and solar variability using best-track data for over three solar cycles. We look into variability across all major regions instead of only NA/US hurricanes. Also special attention is paid to solar cycle dependence of extreme TCs considering their socioeconomically importance.

2. Data and Methodology

2.1. TC Activity

In this study, global TC activity was inferred by using the International Best Track Archive for Climate Stewardship (IBTrACS) Data set v04r for all TC regions (Knapp et al., 2010, 2018). For Sections 3.1 and 3.2, where we look into correlations between TC activity and SSNs, we have used TC data and SSN from 1964 to 2021. This has been done to have a longer time series. For Section 3.3 onward, everywhere throughout the paper, we only consider TCs from 1982 onwards. This has been done since decent satellite coverage and hence more accurate TC intensity data was available after that. In general, only storms with minimum intensity ≥34 knots have been taken into consideration unless stated otherwise. For both cases, all extra-tropical and subtropical storms were ignored. Only storms categorized as TCs have been considered. For TC counts, we have considered all data after 1964, depending on data availability in different regions.

2.2. Accumulated Cyclone Energy (ACE)

Along with TC counts, we have also used the accumulated cyclone energy (ACE) as a proxy for TC activity. The "ACE" index was defined by NOAA as a measure of the total TC activity (Waple et al., 2002). The "ACE" index takes into account both the strength and the time duration of each TC and hence acts as a better proxy for TC activity as compared to just TC counts. For each TC, the "ACE" index is calculated by summing up the squares of each six hourly maximum sustained wind speed (u_{max}) and then multiplying it with a factor of 10^4. Only those periods are considered when $u_{max} \geq 34$ knots. In short, for each TC, $ACE = 10^4 \times \sum v_{max}^2$.

2.3. Sunspot Number (SSN)

As a proxy for solar activity, we have used yearly averaged SSN. The SSN data is obtained from NASA's OMNIWEB service (https://omniweb.gsfc.nasa.gov/). The SSN data is available from 1964 onwards. As mentioned, except for Sections 3.1 and 3.2, everywhere throughout this paper, we have considered TCs after 1982 only. The same goes for SSN data as well. For the period of 1982–2022, the mean SSN is given as $\mu = 75$ and the standard deviation (SD) is $\sigma = 62.6$. At this point, it is necessary to put forth criteria for high and low solar activity conditions. In this case, the high and low solar activity conditions may be defined as $SSN > \mu + \frac{1}{2}\sigma$ and
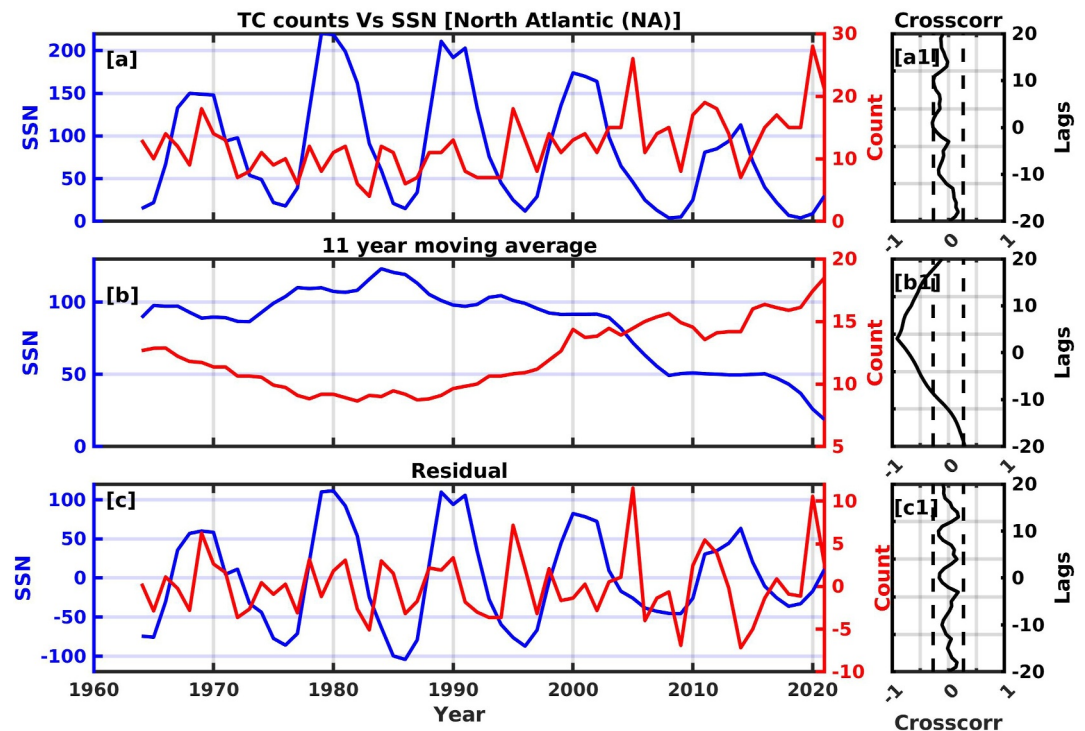
Figure 1. This figure shows the variability of yearly tropical cyclones (TC) counts (red) and the yearly averaged sunspot number (SSN) (blue) over the North Atlantic region. The SSN and TC counts are represented by the left and right *y*-axes, respectively. Panels (a–c) shows the absolute values, their 11-year moving averages, and the residual values (absolute-11-year moving average), for both parameters. Panels (a–c) represent the corresponding cross-correlation functions. The dashed line shows the 95% confidence bounds.

$SSN < \mu - \frac{1}{2}\sigma$, respectively which results in SSN > 106 and SSN < 43. However, for simplicity, we redefine the high and low solar activity conditions as SSN > 100 and SSN < 50. The corresponding results do not change much. So we persist with this criteria of SSN > 100 and SSN < 50 to define high and low solar activity conditions, throughout the paper.

2.4. Probability Distribution Function and Uncertainty Bounds

In Section 3.3, we have used probability distribution functions for TC intensities for low and high solar activity periods. The probabilities are calculated by simply taking the ratio of the number of points in each bin and the total number of points. To calculate the significance levels, we have employed a Monte Carlo bootstrap method. In this method, random noise is added to each data point to create multiple sub-samples. In the IBTrACS data set, the TC intensity is rounded up to the nearest 5 knots. So we produce 10,000 sub-samples by adding random noise from a uniform distribution within the interval of ±5 knots which is a standard error in TC intensity observations. Then the 2.5th–97.5th percentiles of the 10,000 sub-samples were used as the uncertainty bounds. The method employed in this case is very similar to the one used by Bhatia et al. (2019).

In addition, the following abbreviations have been used to denote various regions, throughout this paper: (EP: Eastern pacific, NA: North Atlantic, NI: North Indian, SI: South Indian, SP: South pacific, WP: Western pacific).

3. Results

3.1. TC Counts Versus SSN

Figure 1 shows the variability of yearly TC counts (red) and the yearly averaged SSN (blue) over the NA region. The SSN and TC counts are represented by the left and right *y*-axes, respectively. Figures 1a–1c shows the absolute values, their 11-year moving averages, and the residual values (absolute-11-year moving average), for both parameters. On the right, Figures 1a–1c represent the corresponding cross-correlation functions. The dashed

lines show the 95% confidence bounds. On a visual inspection, Figures 1a–1c do not show any clear relationship between TC counts and SSN. A similar picture is observed in terms of their cross-correlations in Figures 1a–1c. However, Figure 1b show a different picture. A clear visual anti-correlation can be observed between TC counts and SSN when we consider their 11-year moving average. The same is also evident in terms of their cross-correlation which is nearly −1. This points toward a possibility that a higher level of solar activity leads to lower numbers of TCs and vice versa. However, this is a picture of only the NA region. We must take a look at what happens in other regions as well which has been shown in Figure 2.

Figure 2 shows the variation of TC counts (red) and the SSN (blue) in terms of 11-year moving averages, for different regions. Each panel is similar to Figure 1b, except the TC counts in this case are normalized with respect to the maximum value for each region. The SSN and TC counts are represented by the left and right y-axes, respectively. The horizontal panels represent different regions (mentioned in the bottom left corner). The respective cross-correlation coefficients, at zero lag, have been mentioned in the middle bottom for each panel. First of all, the NA region shows strong anti-correlation between TC counts and SSN variability (Figure 2b). However, none of the other regions show such strong anti-correlation. On the contrary, the SP region shows a positive correlation (Figure 2e). Both TC counts and SSN show similar trends on a visual inspection. Overall, in the last two decades, all regions in the northern hemisphere (EP, NA, NI, WP) show a gradual increase in TC counts. Interestingly, the corresponding southern hemispheric regions (SI, SP) show a gradual decreasing trend in TC counts.

3.2. Accumulated Cyclone Energy (ACE) Versus SSN

Figure 3 shows a similar picture in terms of the ACE. Figure 3 is similar to Figure 2 except it shows the variation of the ACE (red) and the SSN (blue) in terms of 11 years moving averages, for different regions. The ACE variability with respect to SSN is very similar to that of TC counts. Similar to Figure 2b, the NA region shows strong anti-correlation between ACE and SSN variability (Figure 3b). None of the other regions show such strong anti-correlation. As mentioned in Section 2, the ACE takes into account both the TC intensity and duration. Hence it is a better physical indicator of TC variability than only TC counts. But when we consider their long-term variability, TC counts and ACE both show very similar behavior in most of the regions. The most prominent one is the NA region where both TC counts and ACE show a strong negative correlation with SSN.

3.3. Distribution of TC Intensities

Figure 4 shows a picture of the distribution of TC intensities under different solar activity conditions. The figure has been generated by using TC data only after 1982. The left panel (Figures 4a–4d) shows the distribution of TC intensities for (a) all solar activity levels (b) low solar activity (SSN < 50) (c) high solar activity conditions (SSN > 100) and (d) difference between low and high solar activity conditions. The y-axis for the top three panels is in linear scale whereas the bottom panel is in log scale. The x-axis shows the TC intensities in knots. The data has been binned into bins of 20 knots each. From Figures 4b and 4c it can be seen that the number of TCs is generally higher during low solar activity conditions which is evident from the difference plotted in Figure 4d. However, this may not be completely correct because the number of years falling under lower solar activity conditions may be higher than that under higher solar activity conditions. So Figures 4e–4g show the TC counts, number of years, and the TC counts/year (yearly rate). The blue, green, and red colors represent low, moderate, and high solar activity levels, respectively. As seen in Figure 4g, the rates are almost similar in all three solar activity conditions. However, the yearly rates do not differentiate the TC intensity. So to understand if the TC intensity has any dependence on the solar activity levels, we take a look at their probability distributions.

Figure 5, shows the corresponding probability distribution functions for low (blue) and high (red) solar activity conditions. The probabilities are represented in a log10 scale in the y-axis whereas the x-axis shows the TC intensity in knots. The solid lines represent the probability distributions whereas the dotted lines represent the 95% confidence intervals which have been calculated using a Monte Carlo simulation as described in Section 2. The probability in this case is simply the ratio between the number of TCs in each bin and the total number of TCs for each category. The probabilities are plotted in log scale to have a better picture of the tail end of the distribution. Overall, the probabilities do not vary much throughout most parts of the distributions. However, the points on the extreme right in the tail end of the distributions, show a clear difference. What it means is that the most intense TCs are more probable during lower solar activity conditions, as compared to higher solar activity conditions.
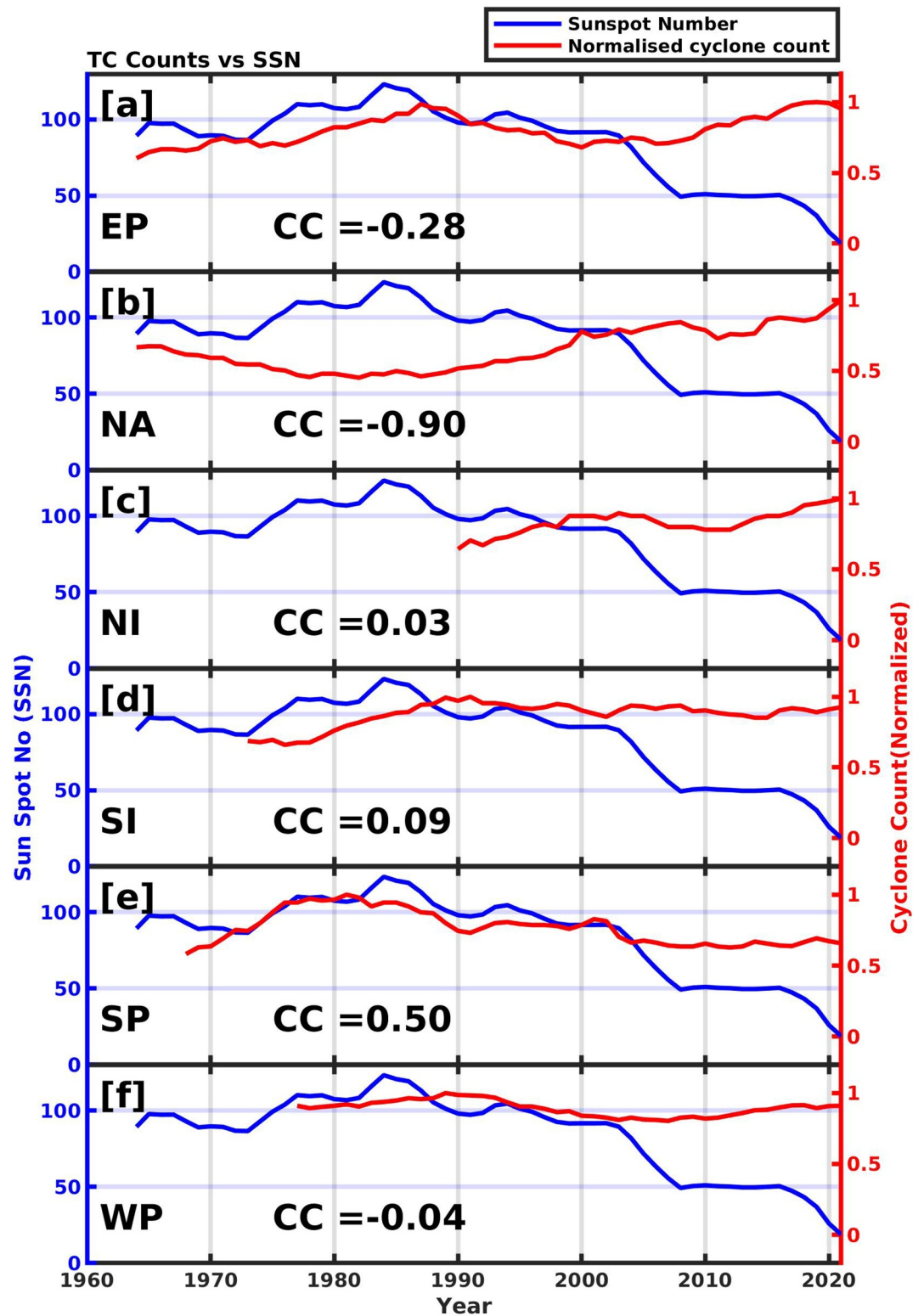
Figure 2. This figure shows the variation of tropical cyclone (TC) counts (red) and the sunspot number (SSN) (blue) in terms of 11 years moving averages, for different regions. Each panel is similar to Figure 1b, except the TC counts in this case are normalized with respect to the maximum value for each region. The SSN and TC counts are represented by the left and right *y*-axes, respectively. The horizontal panels represent different regions (mentioned in the bottom left corner).
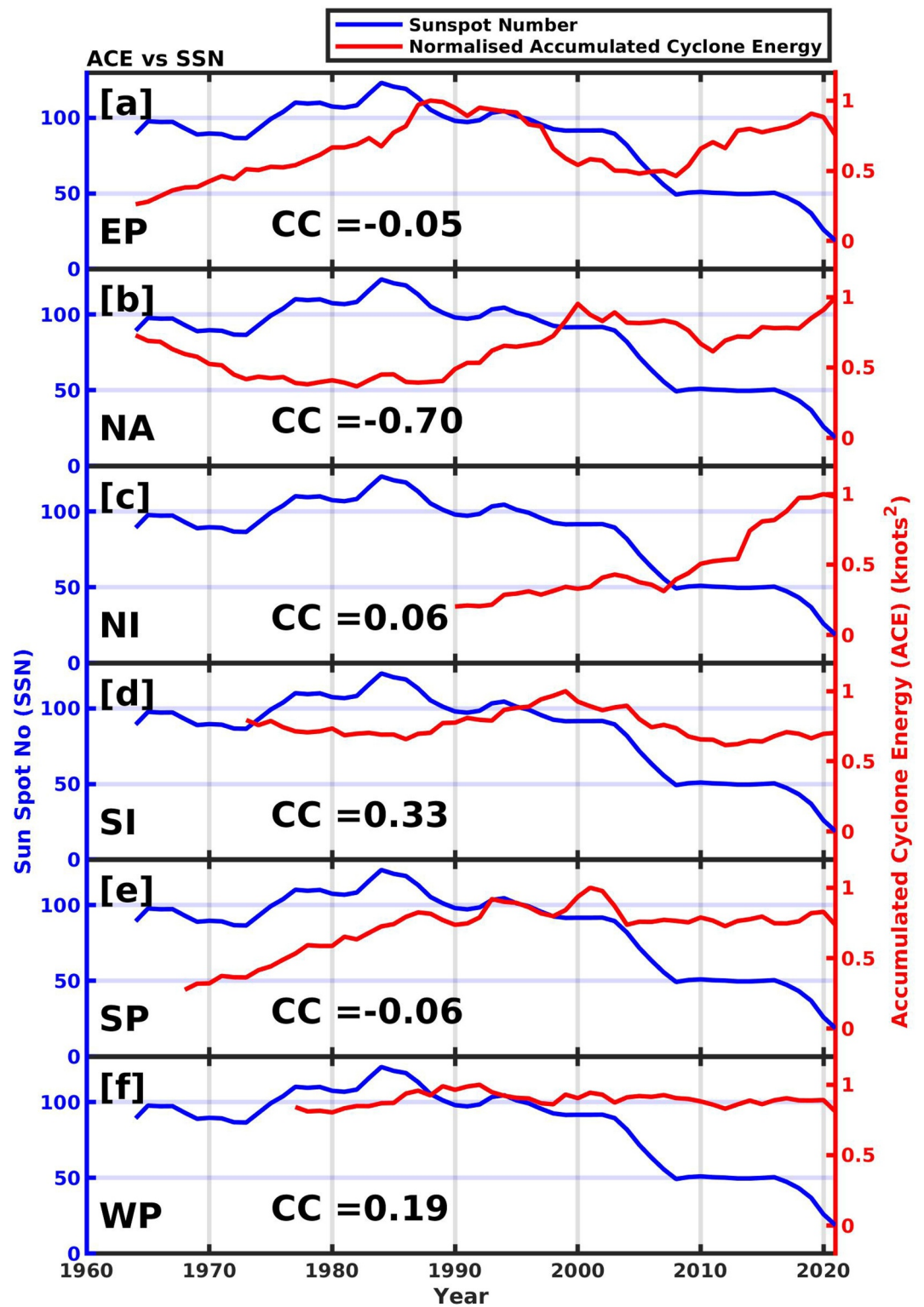
Figure 3. This figure shows the variation of accumulated cyclone energy (ACE) (red) and the sunspot number (blue) in terms of 11 years moving averages, for different regions. This figure is similar to Figure 2 except it shows the variation of the ACE (red) instead of tropical cyclone counts.
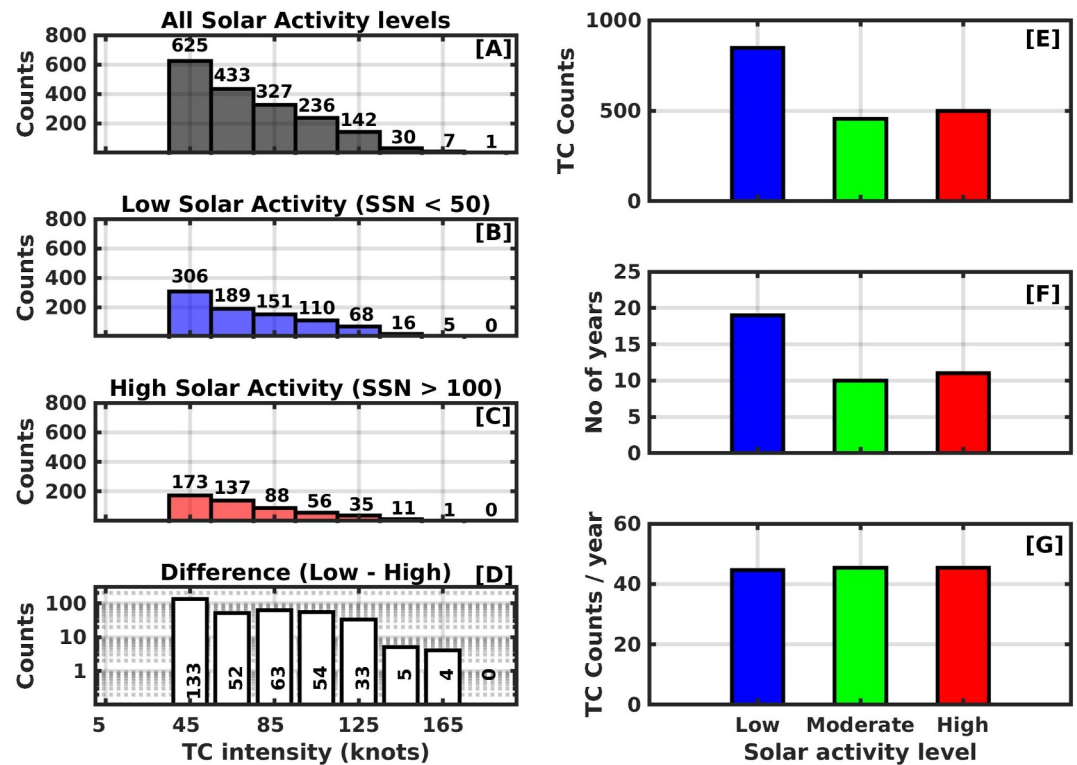
Figure 4. This figure shows a picture of the distribution of tropical cyclone (TC) intensities under different solar activity conditions. The left panel (a–d) shows the distribution of TC intensities for (a) all solar activity levels (b) low solar activity (SSN < 50) (c) high solar activity conditions (SSN > 100) and (d) difference between low and high solar activity conditions. The right panel (e–g) shows (e) TC counts (f) the number of years and (g) TC counts per year under different solar activity conditions.

Considering the importance of highly intense TCs, we look at their variability with respect to solar cycles in the next section.

3.4. Extreme Events

In this section, we consider the occurrence of extreme TC events with respect to solar variability. We define an extreme TC event as a TC with a maximum sustained wind speed of 137 knots or higher (category 5 as per Saffir (1973), Simpson (1974)). Figure 6 shows the occurrence of extreme TCs with $U_{max} \geq 137$ knots. The horizontal panels (Figures 6b–6f) in the left column represent different ocean basins with Figure 6a showing the combination of all regions in a single plot. The black curves show the SSN variation as a function of time (year). The red dots represent the yearly counts of the extreme TCs, with their size representing the number of extreme TCs in a year.

First of all, Figures 6b–6g show that most of the extreme events are confined to the EP and NA regions. Second and more importantly, most of the extreme events occur during lower or moderate solar activity conditions. A very few of the extreme events can be observed to occur around the peak of solar activity. The same scenario is shown in Figure 6h in a slightly different way. The SSN has been divided into three categories: (a) low (SSN < 50), (b) moderate (50 = < SSN < 100), and (c) high (SSN ≥ 100). Then extreme TC count, total number of years, and the extreme TC count per year have been shown in bar plots, for each category, in white, gray, and red bars, respectively, The same has been mentioned in the plots as well. For better visual inspection, the red bars represent 10× (extreme TC count per year). The actual values are mentioned in the text inside the figure, against the red bars. Out of a total of 36 extreme events, 24 occur during lower solar activity conditions (low (SSN < 50)), whereas 4 and 8 extreme events occur during moderate and high solar activity conditions, respectively. It may be argued that the total number of years during lower activity conditions may be higher which leads to a higher number of extreme events. So when we consider the extreme event counts per year, we get 1.3, 0.4, and 0.8
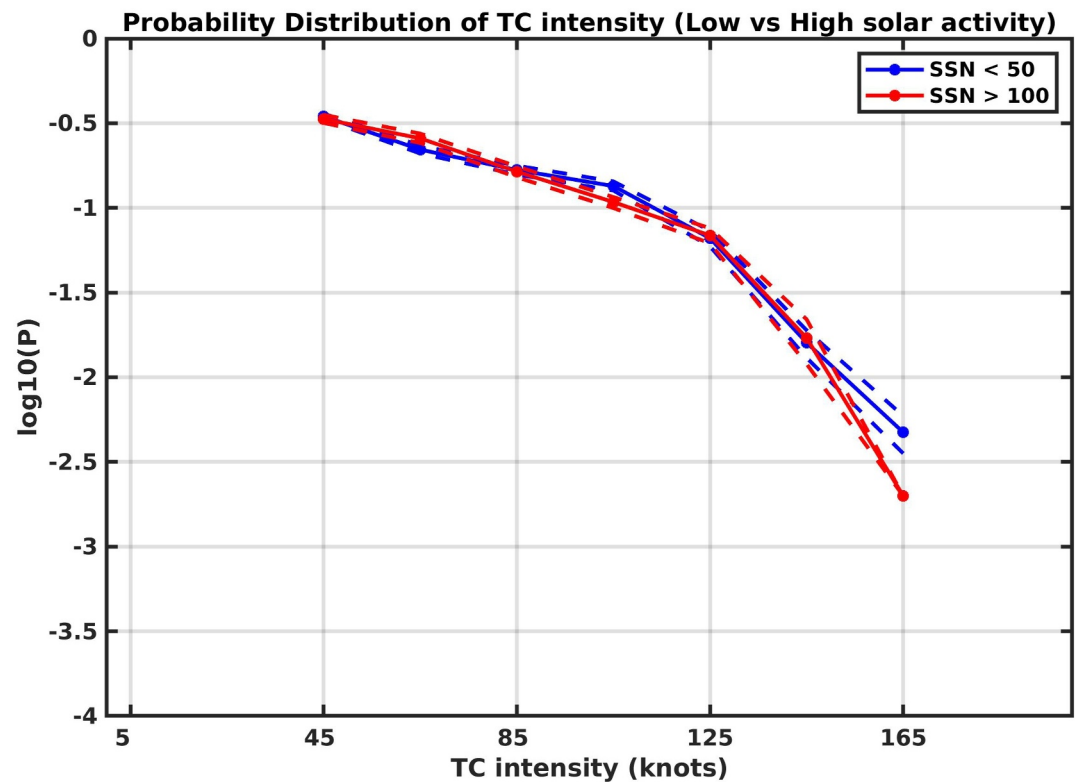
Figure 5. This figure shows the probability distribution functions of tropical cyclone intensity for low (blue) and high (red) solar activity conditions. The probabilities are represented in a log10 scale in the *y*-axis whereas the *x*-axis shows the intensity in knots. The solid lines represent the probability density function whereas the dashed lines represent corresponding 95% confidence intervals.

extreme events per year during low, moderate and high solar activity conditions, respectively. This clearly points toward a higher probability of extreme TC events during lower solar activity conditions.

3.4.1. Extreme Events and Phases of Solar Cycle

To understand the relationship of extreme events with phases of the solar cycle, we first divide each solar cycle into four phases namely, (a) minimum, (b) ascending, (c) maximum, and (d) declining phase (Hynönen, 2013; Kilpua et al., 2015; Reyes et al., 2021). First, a solar cycle is defined from one minimum to the next minimum. Next, the mean and SD are calculated for each cycle. Then the ascending and the declining phases are defined as the regions between Mean $\pm$ 1 SD, on the left and right sides of the solar cycle, respectively. The maximum phase is defined as the region with SSN $\geq$ Mean + 1 SD. Alternatively, the maximum phase lies in between the ascending and the declining phases. The minimum phase is the region where SSN $\leq$ Mean $-$ 1 SD. Alternatively, minimum phase is the combination of regions before the ascending phase and after the declining phase. The different phases of the solar cycle can be seen in Figure 7 as shaded regions with different colors. For creating this plot SSN data from 1982 to 2019 has been used, which covers more than three solar cycles. Each solar cycle was projected onto an *x*–*y* plane where *x* represents an 11-year time period and *y* represents the SSN normalized to 1 with respect to the maximum value of the SSN for that solar cycle. For example, let us consider a 10-year solar cycle with a peak SSN of 200. So the 3rd year with an SSN of 140 will have *x* coordinates $x = (3/10) \times 11 = 3.3$ and $y = 140/200 = 0.7$. The same process was repeated for each solar cycle under consideration and a mean curve is calculated. The results are shown in Figure 7. The black solid curve represents a normalized mean solar cycle of 11 years. The vertical black dashed lines appear as a separation between different phases of the solar cycles. The blue, cyan, yellow, and green represent the minimum, ascending, maximum, and declining phases of a solar cycle. The red circles represent the extreme TC events with the size of the circles representing the number of extreme TCs in that year. The positions of the extreme TCs have been mapped as per their occurrence in their respective phase of the solar cycle. The respective numbers of years and extreme TCs have been mentioned in Table 1. The
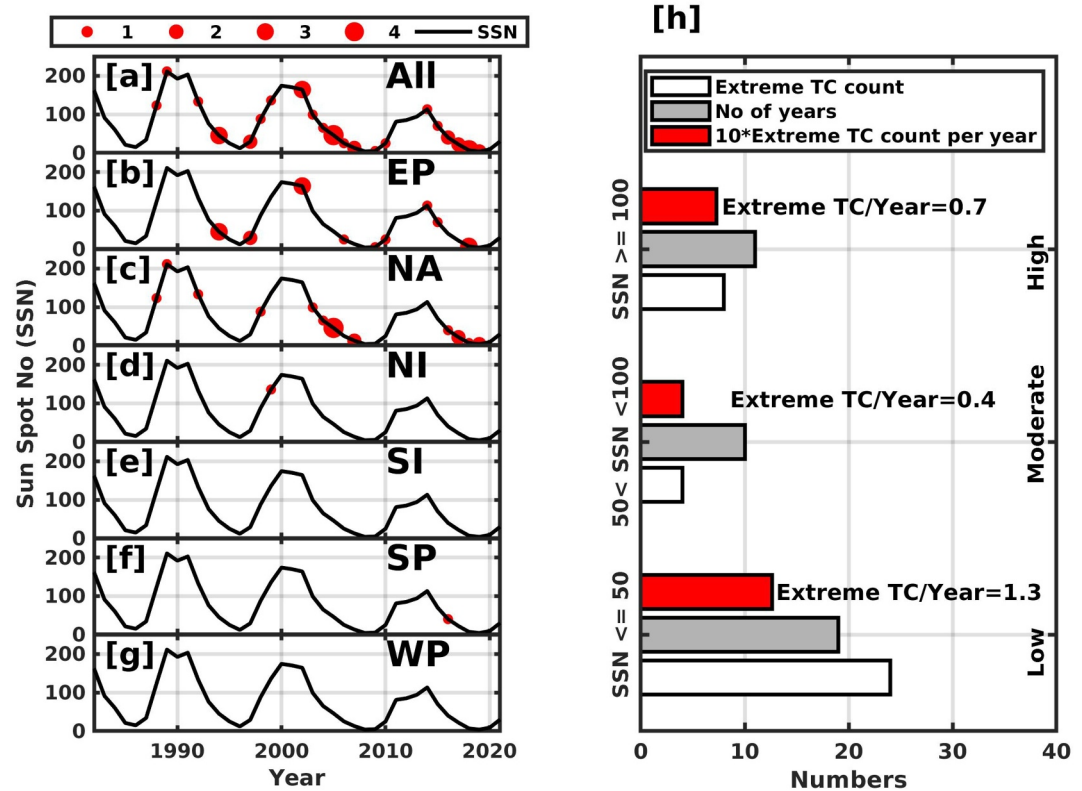
Figure 6. This figure shows the occurrence of extreme tropical cyclone (TCs) with $U_{max} \geq 137$ knots. The horizontal panels in the left column represent different ocean basins with the top panel representing the combination of all. The black curves show the sunspot number (SSN) variation as a function of time (year). The red circles represent the yearly counts of the extreme TCs. The right vertical panel shows extreme TC counts and average yearly counts under different solar activity conditions. The SSN has been divided into three regions based on solar activity level and the number of extreme TCs in each category mentioned in the panel.

most striking feature of Figure 7 is that a majority of the extreme TCs occur during the declining phase of the solar cycle, followed by the minimum phase. They are least likely to occur during the maximum and ascending phases. The yearly average extreme TC during declining phase is 1.23 compared to 0.625 during maximum and 0.75 during ascending phase. The interesting thing to note here is that the solar activity levels (in terms of SSN) are almost similar during ascending and declining phases. So it is surprising to note the much higher preference of extreme TCs toward the declining phase as compared to the ascending phase.

4. Discussion

This study investigated the relationship between TC activity and solar variability using TC best-track data and SSN as respective proxies. In the NA region, strong anti-correlation was observed between 11-year moving averages of TC yearly counts and yearly averaged SSN. When we considered the ACE, it also showed a very similar pattern. The TC counts (and the ACE) increased with declining solar activity and decreased with increasing solar activity. However, other regions did not show any such clear relationship. In the South Pacific, a positive correlation was obtained which shows decreasing TC counts with decreasing solar activity levels. The inverse relationship in the NA region is similar to results shown by Elsner and Jagger (2008). Though other regions do not show such an inverse relation like NA region, the overall global TC counts are generally higher during low solar activity periods as compared to higher solar activity period. The global yearly rates remained more or less similar during different solar activity conditions. However, when we consider only extreme TC events (≥137 knots), the yearly rates are extremely high during low solar activity conditions as compared to high or moderate solar activity conditions.
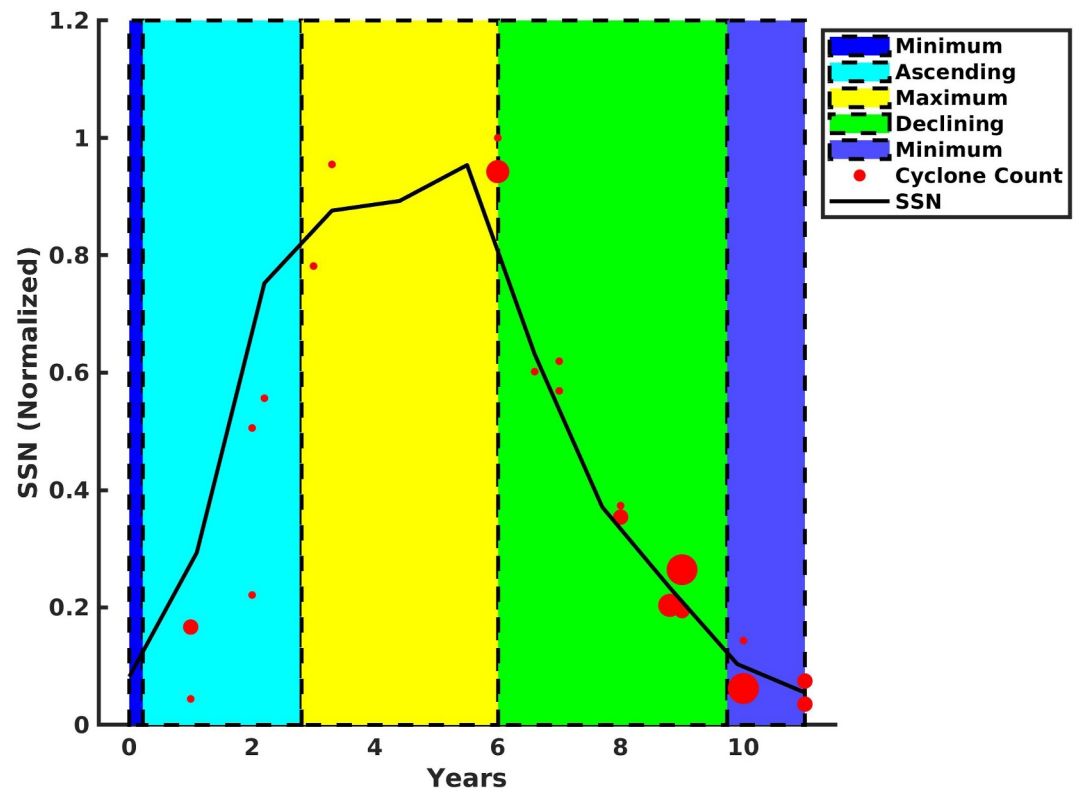
Figure 7. This figure shows the distribution of extreme tropical cyclones (TCs) during different phases of the solar cycle. The black curve shows the mean solar cycle (average of the last three solar cycles under the study) and has been normalized to unity. The red circles represent the yearly counts of the extreme TCs similar to Figure 6. The positions of the extreme TCs have been mapped as per their occurrence in their respective solar cycle. The blue, cyan, yellow, and green represent the minimum, ascending, maximum, and declining phases of a solar cycle. The results show that the extreme TCs are more probable during the declining phases and are least probable during the ascending phases of the solar cycle.

The exact reasons behind the preference of TC activity toward lower solar activity are not very clear. There are very few proposed mechanisms. Elsner et al. (2010) suggested that the decrease in UV radiation during solar minimum conditions may be the main culprit behind the increased TC intensity. As per the heat engine theory of TCs, the maximum wind speed of a TC varies directly with the sea surface temperature (SST) but inversely with the mean outflow temperature on top of the cyclone (K. A. Emanuel, 1991; K. Emanuel, 2023; Elsner et al., 2010). So during high solar activity conditions, the increased UV radiation leads to a hotter upper troposphere. This in turn leads to less available convective potential energy for the TCs and hence weaker TCs. It may be argued at this point that this explanation should result in stronger/weaker TCs during low/high solar activity conditions without really affecting their counts/frequency of occurrence. We must note that the TC counts are not exclusively independent of TC intensity as we define a cut-off value to consider and storm as a TC. For example, in our case, the cut-off is 34 knots. The same was also pointed out by Elsner and Jagger (2008). Elsner et al. (2010) also suggested that the UV-driven change in upper tropospheric temperature is a more significant driver than cosmic variability during a solar cycle when it comes to affecting cyclone intensity. The above-mentioned argument may well explain the results obtained in this study. We must reiterate here that the results from Elsner and Jagger (2008) were limited to only the NA sector.

However, a contrasting mechanism was proposed by Li et al. (2019). The authors investigated the variability of TC activity with reference to solar wind energy input during a solar cycle and concluded that intense geomagnetic activity may lead to stronger TCs. They explained the results

Table 1
Extreme Tropical Cyclones (TCs) Versus Solar Cycle Phases

Solar cycle phase	No of years	No of extreme TCs	Extreme TC/year
Minimum	9	9	1
Ascending	8	6	0.75
Maximum	8	5	0.625
Declining	13	16	1.23

considering the variability of cosmic rays during the solar cycle as a major driver. It has been established that there is a strong anti-correlation between the 11-year solar cycle and cosmic ray intensity (Forbush, 1958; Parker, 1965; Van Allen, 2000). As the solar activity peaks, the cosmic ray intensity drops resulting in a decreased flux of cosmic ray particles that reach the troposphere. Past studies have positively linked cosmic rays flux with global cloud coverage (Lassen & Friis-Christensen, 1995; Svensmark & Friis-Christensen, 1997). The reduced cosmic ray flux during high solar activity leads to a decrease in global cloud coverage which may allow the open oceans to absorb more solar irradiance energy. As a result, the SST and the latent heat increase. Increased SST and latent heat act as a source of energy for TCs to get further intensified (Pauley & Smith, 1988).

Other than the two competing mechanisms discussed above, there are hardly any other physical mechanisms that discuss or explain the relationships between solar and TC activity variability. Our results are agreeable to the mechanism suggested by Elsner et al. (2010), Elsner and Jagger (2008). However, the mechanism discussed by Li et al. (2019) cannot be completely negated. Both the mechanisms may in principle be valid although their degree of significance in driving the solar-TC relationship may vary.

When we consider only the extreme TC events, they are clearly more probable to occur during years with lower solar activity with an average of 1.3 extreme events per year compared to 0.7 and 0,4 extreme events per year during high and moderate solar activity. Perhaps the most important result of this study is the discovery that extreme TC events are least likely to occur during the maximum and ascending phases of a solar cycle. They are most likely to occur during the declining phase. Although the solar activity levels are similar during the ascending and declining phases of a solar cycle, the extreme TC event occurrence rate is almost double during the declining phase rather than during the ascending phase. It may be easier to look for driving mechanisms when we separately look at low and high solar activity conditions. When we compare the ascending and descending phases of a solar cycle, they are very similar in terms of SSN. So at first, it is surprising to observe that extreme TCs are far more probable during the declining phase as compared to the ascending phase of a solar cycle. The only difference lies in their preconditioning. An ascending phase is preceded by a solar minimum whereas a declining phase is preceded by a solar maximum. However, at this point, we do not have any probable mechanism to explain why the ascending phases are least preferred for an extreme TC to occur.

5. Conclusion

We have studied the relationship between solar activity and TC activity. The study utilized SSN as a proxy for solar activity. TC activity was inferred from IBTrACS data set The major findings are as follows.

1. The long-term trends in TC occurrence and SSN suggest that, in the Northern Atlantic region, solar activity and TC activity are strongly anti-correlated. TC occurrence count increases with decreasing solar activity and vice versa. A similar behavior is observed in terms of ACE.
2. Lower solar activity conditions are more favorable toward the generation of more intense TCs as compared to those in higher solar activity.
3. More importantly, extreme TC events (≥ 137 knots) are most likely to occur during the declining phase of a solar cycle. They are least probable during the maximum and ascending phases of the solar cycle.
4. Although solar activity levels are similar during the declining and ascending phases, the yearly occurrence rate is nearly double in the declining phase (1.123) as compared to that in the ascending phase (0.625).

The exact physics and dynamics behind such behavior are not clearly understood. It would require a proper modeling framework to understand and explain how solar variability controls/contributes toward TC activity.

Data Availability Statement

The IBTrACS data can be downloaded from the IBTrACS website https://www.ncei.noaa.gov/products/international-best-track-archive. The SSN data can be obtained from NASA's OMNIWEB service https://omniweb.gsfc.nasa.gov/. The datasets for this research can be found at Nayak (2024).

References

Bhatia, K. T., Vecchi, G. A., Knutson, T. R., Murakami, H., Kossin, J., Dixon, K. W., & Whitlock, C. E. (2019). Recent increases in tropical cyclone intensification rates. *Nature Communications*, *10*(1), 635. https://doi.org/10.1038/s41467-019-08471-z

Chan, J. C. (2005). The physics of tropical cyclone motion. *Annual Review of Fluid Mechanics*, *37*(1), 99–128. https://doi.org/10.1146/annurev.fluid.37.061903.175702

Chen, R., Zhang, W., & Wang, X. (2020). Machine learning in tropical cyclone forecast modeling: A review. *Atmosphere*, *11*(7), 676. https://doi.org/10.3390/atmos11070676

Cohen, T., & Sweetser, E. (1975). The spectra of the solar cycle and of data for Atlantic tropical cyclones. *Nature*, *256*(5515), 295–296. https://doi.org/10.1038/256295a0

Elsner, J. B., & Jagger, T. H. (2008). United States and Caribbean tropical cyclone activity related to the solar cycle. *Geophysical Research Letters*, *35*(18), L18705. https://doi.org/10.1029/2008GL034431

Elsner, J. B., Jagger, T. H., & Hodges, R. E. (2010). Daily tropical cyclone intensity response to solar ultraviolet radiation: Hurricane intensity and the solar activity. *Geophysical Research Letters*, *37*(9), L09701. https://doi.org/10.1029/2010GL043091

Emanuel, K. (2003). Tropical cyclones. *Annual Review of Earth and Planetary Sciences*, *31*(1), 75–104. https://doi.org/10.1146/annurev.earth.31.100901.141259

Emanuel, K. (2023). *Atmospheric convection*. Oxford University Press.

Emanuel, K. A. (1991). The theory of hurricanes. *Annual Review of Fluid Mechanics*, *23*(1), 179–196. https://doi.org/10.1146/annurev.fl.23.010191.001143

Forbush, S. E. (1958). Cosmic-ray intensity variations during two solar cycles. *Journal of Geophysical Research*, *63*(4), 651–669. https://doi.org/10.1029/JZ063i004p00651

Ge, X., Ma, Y., Zhou, S., & Li, T. (2015). Sensitivity of the warm core of tropical cyclones to solar radiation. *Advances in Atmospheric Sciences*, *32*(8), 1038–1048. https://doi.org/10.1007/s00376-014-4206-0

Haig, J. E., & Nott, J. (2016). Solar forcing over the last 1500 years and Australian tropical cyclone activity. *Geophysical Research Letters*, *43*(6), 2843–2850. https://doi.org/10.1002/2016GL068012

Hines, C. O., & Halevy, I. (1977). On the reality and nature of a certain sun-weather correlation. *Journal of the Atmospheric Sciences*, *34*(2), 382–404. https://doi.org/10.1175/1520-0469(1977)034⟨0382:OTRANO⟩2.0.CO;2

Hynönen, R. (2013). *Geomagnetic activity and its sources during modern solar maximum*. Master's thesis. University of Helsinki.

Ivanov, K. G. (2007). Correlation between tropical cyclones and magnetic storms during cycle 23 of solar activity. *Geomagnetism and Aeronomy*, *47*(3), 371–374. https://doi.org/10.1134/S0016793207030140

Kilpua, E. K. J., Olspert, N., Grigorievskiy, A., Käpylä, M. J., Tanskanen, E. I., Miyahara, H., et al. (2015). Statistical study of strong and extreme geomagnetic disturbances and solar cycle characteristics. *The Astrophysical Journal*, *806*(2), 272. https://doi.org/10.1088/0004-637X/806/2/272

Knapp, K. R., Diamond, H. J., Kossin, J. P., Kruk, M. C., & Schreck, C. J. (2018). *International best track archive for climate stewardship (Ibtracs) project, version 4. International best track archive for climate stewardship (Ibtracs) project, version 4*. NOAA National Centers for Environmental Information. https://doi.org/10.25921/82ty-9e16

Knapp, K. R., Kruk, M. C., Levinson, D. H., Diamond, H. J., & Neumann, C. J. (2010). The international best track archive for climate stewardship (Ibtracs): Unifying tropical cyclone best track data. *Bulletin of the American Meteorological Society*, *91*(3), 363–376. https://doi.org/10.1175/2009BAMS2755.1

Lassen, K., & Friis-Christensen, E. (1995). Variability of the solar cycle length during the past five centuries and the apparent association with terrestrial climate. *Journal of Atmospheric and Terrestrial Physics*, *57*(8), 835–845. https://doi.org/10.1016/0021-9169(94)00088-6

Li, H., Wang, C., He, S., Wang, H., Tu, C., Xu, J., et al. (2019). Plausible modulation of solar wind energy flux input on global tropical cyclone activity. *Journal of Atmospheric and Solar-Terrestrial Physics*, *192*, 104775. https://doi.org/10.1016/j.jastp.2018.01.018

Nayak, C. (2024). Datasets for the draft effects of solar variability on tropical cyclone activity [Dataset]. *Zenedo*. https://doi.org/10.5281/zenodo.10448316

Parker, E. (1965). The passage of energetic charged particles through interplanetary space. *Planetary and Space Science*, *13*(1), 9–49. https://doi.org/10.1016/0032-0633(65)90131-5

Pauley, P. M., & Smith, P. J. (1988). Direct and indirect effects of latent heat release on a synoptic-scale wave system. *Monthly Weather Review*, *116*(5), 1209–1236. https://doi.org/10.1175/1520-0493(1988)116⟨1209:DAIEOL⟩2.0.CO;2

Prikryl, P., Bruntz, R., Tsukijihara, T., Iwao, K., Muldrew, D. B., Rušin, V., et al. (2018). Tropospheric weather influenced by solar wind through atmospheric vertical coupling downward control. *Journal of Atmospheric and Solar-Terrestrial Physics*, *171*, 94–110. https://doi.org/10.1016/j.jastp.2017.07.023

Prikryl, P., Iwao, K., Muldrew, D. B., Rušin, V., Rybanský, M., & Bruntz, R. (2016). A link between high-speed solar wind streams and explosive extratropical cyclones. *Journal of Atmospheric and Solar-Terrestrial Physics*, *149*, 219–231. https://doi.org/10.1016/j.jastp.2016.04.002

Prikryl, P., Muldrew, D. B., & Sofko, G. J. (2009). The influence of solar wind on extratropical cyclones—Part 2: A link mediated by auroral atmospheric gravity waves? *Annales Geophysicae*, *27*(1), 31–57. https://doi.org/10.5194/angeo-27-31-2009

Prikryl, P., Rušin, V., & Rybanský, M. (2009). The influence of solar wind on extratropical cyclones—Part 1: Wilcox effect revisited. *Annales Geophysicae*, *27*(1), 1–30. https://doi.org/10.5194/angeo-27-1-2009

Reyes, P. I., Pinto, V. A., & Moya, P. S. (2021). Geomagnetic storm occurrence and their relation with solar cycle phases. *Space Weather*, *19*(9), e2021SW002766. https://doi.org/10.1029/2021SW002766

Roberts, W. O., & Olson, R. H. (1973). Geomagnetic storms and wintertime 300-mb trough development in the north pacific-North America area. *Journal of the Atmospheric Sciences*, *30*(1), 135–140. https://doi.org/10.1175/1520-0469(1973)030⟨0135:GSAWMT⟩2.0.CO;2

Roy, C., & Kovordányi, R. (2012). Tropical cyclone track forecasting techniques—A review. *Atmospheric Research*, *104–105*, 40–69. https://doi.org/10.1016/j.atmosres.2011.09.012

Saffir, H. S. (1973). Hurricane wind and storm surge. *The Military Engineer*, *423*, 4–5.

Simpson, R. H. (1974). The hurricane disaster potential scale. *Weatherwise*, *27*, 169–186. https://doi.org/10.1080/00431672.1974.9931702

Svensmark, H., & Friis-Christensen, E. (1997). Variation of cosmic ray flux and global cloud coverage—A missing link in solar-climate relationships. *Journal of Atmospheric and Solar-Terrestrial Physics*, *59*(11), 1225–1232. https://doi.org/10.1016/S1364-6826(97)00001-1

Van Allen, J. A. (2000). On the modulation of galactic cosmic ray intensity during solar activity cycles 19, 20, 21, 22 and early 23. *Geophysical Research Letters*, *27*(16), 2453–2456. https://doi.org/10.1029/2000GL003792

Wang, Y., & Wu, C.-C. (2004). Current understanding of tropical cyclone structure and intensity changes—A review. *Meteorology and Atmospheric Physics*, *87*(4), 257–278. https://doi.org/10.1007/s00703-003-0055-6

Waple, A. M., Lawrimore, J. H., Halpert, M. S., Bell, G. D., Higgins, W., Lyon, B., et al. (2002). Climate assessment for 2001. *Bulletin of the American Meteorological Society*, *83*(6), S1–S62. https://doi.org/10.1175/1520-0477(2002)083<0938:caf>2.3.co;2

Wilcox, J. M., Scherrer, P. H., Svalgaard, L., Roberts, W. O., & Olson, R. H. (1973). Solar magnetic sector structure: Relation to circulation of the earth's atmosphere. *Science*, *180*(4082), 185–186. https://doi.org/10.1126/science.180.4082.185

Wilcox, J. M., Scherrer, P. H., Svalgaard, L., Roberts, W. O., Olson, R. H., & Jenne, R. L. (1974). Influence of solar magnetic sector structure on terrestrial atmospheric vorticity. *Journal of the Atmospheric Sciences*, *31*(2), 581–588. https://doi.org/10.1175/1520-0469(1974)031⟨0581:IOSMSS⟩2.0.CO;2

Wilcox, J. M., Svalgaard, L., & Scherrer, P. H. (1976). On the reality of a sun-weather effect. *Journal of the Atmospheric Sciences*, *33*(6), 1113–1116. https://doi.org/10.1175/1520-0469(1976)033⟨1113:OTROAS⟩2.0.CO;2